THE INFLUENCE OF UNSTEADY AERODYNAMICS ON THE FREQUENCY-RESPONSE OF A HOVERING ROTOR

Aviv Rosen
Faculty of Aerospace Eng.
Technion-Israel Institute of Technology
Haifa 32000, Israel

Abstract

A recently developed new unsteady aerodynamic model of a hovering rotor (TEMURA) is used to investigate the influence of unsteady aerodynamic effects of the frequency-response of a hovering rotor. The study includes four bladed hingeless rotors that differ in their first rotating flapping frequency. The influence of various effects is investigated and discussed. In general variations in the intensity of the circulation of the trailing vortices have the largest influence. The theoretical results exhibit good agreement with experimental results from the literature.

1. Introduction

The frequency-response of a helicopter is very important in flight dynamics (Ref. 1). During recent years, through the efforts of Tischler and others (for example Refs. 2, 3) frequency-response has become a standard tool for the identification of helicopter and rotor characteristics. Frequency-response is also very important in helicopter dynamics and aeroelasticity (Ref. 4). Since frequency-response is associated with fast variations of the blades' velocities and angles, accompanied by fast variations of the aerodynamic loads along the blades, it is clear that unsteady aerodynamic effects should be included in the analysis of rotor frequency response, in order to obtain good accuracy. Thus, various unsteady aerodynamic models were applied, immediately after their derivation, to the analysis of the frequency-response of rotors.

Loewy (Ref. 5) derived a two-dimensional vortex model of rotor unsteady aerodynamics, that describes the influence of the shed vortices in the returning wake below the rotor. Immediately after its publication this model was applied (Ref. 6) to the analysis of the flapping response of a hovering two-bladed rotor to vertical hub oscillations. The new model succeeded in explaining the decrease in the damping at high frequencies. Similar results were obtained in (Ref. 7) where the damping of symmetric flapwise bending modes of a two-bladed teetering and flapping rotor were measured and compared with theoretical results. In later investigations Loewy's model succeeded in improving the correlations between theoretical and experimental results for the thrust frequency-response (of a hovering rotor) to vertical hub oscillations (Ref. 8), or to collective pitch oscillations (Ref. 9).

Dynamic-inflow models (Refs. 10,11) offer approximate representation of unsteady rotor aerodynamics. These models have been successful in improving the agreement between various frequency-response calculations and experimental results. The studies included:
- Pitch and roll moments transferred from a hingeless rotor to the hub as a result of shaft roll and pitch oscillations or cyclic pitch oscillations (Ref. 12 also see 10 and 13).
- Flapping response to blades' pitch angle oscillations (Ref. 14).
- Roll or pitch rate response of a helicopter to cyclic pitch oscillations (Ref. 15).

After the presentation of the influence of geometric effects (deformation of the wake) due to pitch or roll, on rotor unsteady aerodynamics (Ref. 16), dynamic-inflow models were extended to include the new phenomenon (Refs. 17, 18). It was shown (Ref. 18) that the correlation between calculated and experimental results, for helicopter pitch and roll rate frequency-response to cyclic pitch, improves as a result of including geometric effects.

Recently a model of unsteady airfoil aerodynamics (Ref. 19) was applied (Ref. 20) to investigate a helicopter roll-rate frequency-response to longitudinal and lateral cyclic input. Relatively small influences were observed, that slightly improved the correlation with flight test results.

In an effort to account for unsteady aerodynamic effects that are not taken into account otherwise, an aerodynamic phase-lag was introduced in Refs. 21, 22. As a result the off-axis frequency-response was predicted correctly.

Recently a new detailed unsteady aerodynamic model of a hovering helicopter was presented (Refs. 16, 23-25). This is a vortex model that takes into account the influence of bound, trailing and shed vortices, together with geometric effects. The new model is called TEMURA (Technion Model of Unsteady Rotor Aerodynamics) and succeeded in explaining the off-axis response of a pitching rotor (Ref. 16), predicting the flapping response of a rotor (Ref. 26), analyzing the coupled rotor/body dynamics (Refs. 27, 28) and calculating the pitch damping of rigid rotors (Refs. 29).

Until now TEMURA was applied for frequency-response analysis only in the case of flapping response to blades' harmonic pitch variations (Ref. 26). In the present paper the model will be used for a detailed frequency-response analysis of a hovering

rotor. The pitch and roll moments that are transferred to the rotor hub of a hovering rotor, as a result of pitch or roll oscillations of the shaft, or harmonic variations of the cyclic pitch, will be studied. The influence of rotor stiffness and the frequency of the harmonic variation will be investigated. In addition the relative influence of various parts of the model will be studied including: trailing vortices, shed vortices, and geometric effects.

2. Theoretical Background

In Ref. 27 (for more details see Ref. 30, while Ref. 28 presents a very brief description) the equations of motion of a rotor-body system in hover were presented. It was assumed that the basic state of hover is "symmetric", namely: there are no azimuthal variations in the behavior of the blades and the body pitch and roll angles are equal to zero. The perturbations about the basic state include (τ is time):

$\widetilde{\beta}_c(1,\tau)$, $\widetilde{\beta}_s(1,\tau)$ - The first cosine and sines multiblade flapping coordinates, respectively. The first one is positive if the blade is above the hub plane when it passes over the tail. The second one is positive if the blade is above the hub plane when it points to the right.

$\widetilde{\alpha}$, $\widetilde{\phi}$ - The body pitch and roll angles, respectively, $\widetilde{\alpha}$ is positive when nose-up, $\widetilde{\phi}$ is positive for right roll.

$\widetilde{\theta}(n,\tau)$ - The perturbation in the pitch angle of the nth blade at time τ, that is superimposed on the basic collective pitch angle, θ_0.

It should be noted that the notation $\widetilde{\alpha}$ and $\widetilde{\phi}$ replaces the original notation, φ_p and φ_r, respectively, in Refs. 27, 28 and 30.

It is assumed the $\widetilde{\theta}(n,\tau)$ is the result of cyclic pitch variations, namely:

$$\widetilde{\theta}(n,\rho,\tau) = -\widetilde{A}_1(\tau)\cdot\cos\psi(n,\tau) - \widetilde{B}_1(\tau)\cdot\sin\psi(n,\tau) \tag{1}$$

$\psi(n,\tau)$ is the azimuth angle of blade n at time τ and is equal to zero over the tail.

The analysis is confined to harmonic perturbations. Since a frequency-response of a linear system is considered, it can be assumed that all the perturbations in the non-rotating system oscillate with the same angular frequency, λ. It is convenient to use complex algebra where perturbations in the non-rotating system are described, as follows:

$$\widetilde{A}(...,\tau) = Re[\widetilde{A}(....)\cdot e^{i\cdot\lambda\cdot\tau}] \tag{2}$$

$\widetilde{A}$ represents any one of the perturbations. $\widetilde{A}(...)$ is a complex amplitude that is not a function of time, but represents amplitude and phase shift.

A control vector $\{\widetilde{u}\}$ is defined:

$$\{\widetilde{u}\} = \{\widetilde{\widetilde{u}}\}\cdot e^{i\cdot\lambda\cdot\tau} \tag{3}$$

where:

$$\{\widetilde{\widetilde{u}}\} = \left[\widetilde{\widetilde{A}}_1, \widetilde{\widetilde{B}}_1\right]^T \tag{4}$$

A response vector $\{\widetilde{y}\}$ is also defined:

$$\{\widetilde{y}\} = \{\widetilde{\widetilde{y}}\}\cdot e^{i\cdot\lambda\cdot\tau} \tag{5}$$

where:

$$\{\widetilde{\widetilde{y}}\} = \left[\widetilde{\widetilde{\beta}}_c, \widetilde{\widetilde{\beta}}_s, \widetilde{\widetilde{\alpha}}, \widetilde{\widetilde{\phi}}\right]^T \tag{6}$$

In Refs. 27, 28, 30 the following equation is obtained:

$$[H_3]\{\widetilde{\widetilde{y}}\} = [H_4]\{\widetilde{\widetilde{u}}\} \tag{7}$$

where $[H_3]$ and $[H_4]$ are complex matrices of order (4x4) and (4x2), respectively. These matrices are functions of the rotor-body properties, mode of operation and frequency of oscillations.

In many cases the frequency-response to harmonic variations of the cyclic stick position are of interest. If $\widetilde{\widetilde{\delta}}_{lon}$ and $\widetilde{\widetilde{\delta}}_{lat}$ are the complex amplitudes of the longitudinal and lateral stick commands, respectively, then it is convenient to use the following equation:

$$\{\widetilde{\widetilde{u}}\} = [U_g]\{\widetilde{\widetilde{u}}_p\} \tag{8}$$

where:

$$\{\widetilde{\widetilde{u}}_p\} = \left[\widetilde{\widetilde{\delta}}_{lat}, \widetilde{\widetilde{\delta}}_{lon}\right]^T \tag{9}$$

$[U_g]$ is a gearing square matrix of order 2.

Substitution of Eq. (8) into Eq. (7) results in:

$$[H_3]\{\widetilde{\widetilde{y}}\} = [H_5]\{\widetilde{\widetilde{u}}_p\} \tag{10}$$

where $[H_5]$ is a complex matrix of order (4x2), defined as:

$$[H_5] = [H_4][U_g] \tag{11}$$

It is convenient to describe the matrices $[H_3]$ and $[H_5]$ as comprised of complex, square, submatrices of order 2:

$$[H_3] = \begin{bmatrix} [H_{31}] & [H_{32}] \\ [H_{33}] & [H_{34}] \end{bmatrix} \tag{12a}$$

$$[H_5] = \begin{bmatrix} [H_{51}] \\ [H_{52}] \end{bmatrix} \qquad (12b)$$

The moment that is transferred from the rotor to the body, is of prime interest here. This moment is described by its two component: the pitch moment, M_R, about the pitch axis (positive when nose up) and the roll moment, L_R, about the roll axis (positive to the right). It is assumed that the pitch and roll axes are located on the rotor shaft axis, at a distance h below the hub center.

In order to use Eq. (10) to calculate the moments that are transferred from the rotor to the helicopter body, one has to cancel the contributions of moments about the pitch and roll axes, that originate from sources other than the rotor. This is done by canceling the springs that exert restoring pitch and roll moments on the body ($k_p = k_r = 0$, see Refs. (27, 28, 30)), canceling the viscous dampers that exert damping pitch and roll moments on the body ($C_p = C_r = 0$), and canceling the inertial pitch and roll moments that act on the body ($I_p = I_r = 0$).

If all the above mentioned effects are canceled, the following matrix equation is obtained:

$$\left\{ \begin{matrix} \widetilde{M} \\ \widetilde{L} \end{matrix} \right\} = [S] \left\{ \begin{matrix} \widetilde{\alpha} \\ \widetilde{\phi} \end{matrix} \right\} + [C] \{ \widetilde{u}_p \} \qquad (13)$$

where:

$$[S] = [J_{mat}][H_{33}][H_{31}]^{-1}[H_{32}] - [J_{mat}][H_{34}] \qquad (14)$$

$$[C] = [J_{mat}][H_{52}] - [J_{mat}][H_{33}][H_{31}]^{-1}[H_{51}] \qquad (15)$$

$$[J_{mat}] = \begin{bmatrix} J_p & 0 \\ 0 & J_r \end{bmatrix} \qquad (16)$$

J_p and J_r in the last equation are the components of the rotor moment of inertia about the pitch and roll axes, respectively.

The terms of the matrices [S] and [C] represent the frequency-response of the pitch and roll moments (that are transferred from the rotor to the body), to shaft pitch or roll oscillations, or to longitudinal and lateral commands:

$$[S] = \begin{bmatrix} \dfrac{\partial M}{\partial \alpha} & \dfrac{\partial M}{\partial \phi} \\ \dfrac{\partial L}{\partial \alpha} & \dfrac{\partial L}{\partial \phi} \end{bmatrix} \qquad (17a)$$

$$[C] = \begin{bmatrix} \dfrac{\partial M}{\partial \delta_{lat}} & \dfrac{\partial M}{\partial \delta_{lon}} \\ \dfrac{\partial L}{\partial \delta_{lat}} & \dfrac{\partial M_L}{\partial \delta_{lon}} \end{bmatrix} \qquad (17b)$$

3. Frequency-Response of Hingeless Rotors

A detailed experimental research on the frequency-response of hingeless rotors is reported in Refs. 31-33. The experiments included hover and forward flight, but in what follows only hover will be considered. Two geometrically identical, four bladed rotors, were tested. They only differed in the stiffness of the elastic joint between the blade and the hub. By changing the rotor angular speed it was possible to change the first flapping frequency of the rotating blade. P is the ratio between the first flapping frequency of the rotating blade and the rotor angular speed, Ω. In what follows results for P=1.15, 1.28, 1.33 and 1.56 will be presented and discussed.

The theoretical model assumes a rigid blade that is connected to the hub at a certain offset, through a flapping spring. The blade properties, offset and flapping spring constant are determined such that they will optimally match the actual hingeless blade properties and the first flapping frequency of the rotating blade.

The cyclic pitch in (Refs. 31-32) is defined as:

$$\widetilde{\theta}(n,\tau) = \theta_c(\tau) \cdot \cos \psi(n,\tau) + \theta_s(\tau) \cdot \sin \psi(n,\tau) \quad (18)$$

Based on Eqs. (1), (8) and (18), the gearing matrix $[U_g]$ is a diagonal matrix with the terms on the diagonal equal to -1, while:

$$\{ U_p \} = [\theta_c, \theta_s]^T \qquad (19)$$

Instead of the dimensional pitch and roll moments themselves, the pitch and roll moments coefficients, C_m and C_ℓ, respectively, will be considered

$$C_m = M_R / \rho \pi R^4 \Omega^2; \qquad C_\ell = L_R / \rho \pi R^4 \Omega^2 \quad (20)$$

R is the rotor radius.

C_m and C_ℓ will also be normalized by the cross-sectional lift curve slope, a (equal to 5.73), and the rotor solidity, σ (equal to 0.127).

Since the hovering case is "symmetric", the two terms on the diagonal of each of the matrices [C] and [D] are identical. The off-diagonal terms equal in their amplitude and are also identical in the phase angle or exhibit a difference of 180°. Thus, instead of considering the four terms of each matrix, it is sufficient to consider one diagonal term and one off-diagonal. Since the experimental results of the response to roll variations were found to be of a better accuracy (see Ref. 32, p. 60) the second column of the

matrix [S] will be considered and discussed. For the hover case only experimental results for θ_s variations are given in Refs. (32-33), therefore only the terms on the second column of the matrix [C] will be dealt with.

In Refs. (32-33) experimental results for the moment at the hub center are given. Thus in the calculations h (the distance from the hub center to the pitch and roll axes) is taken equal to zero. Actually pitch and roll oscillations were performed about axes that were located at a relatively short distance below the hub center. This distance results in, in addition to angular motions, linear lateral motions of the rotor, that are not taken into account. Analysis shows that the influence of these lateral motions is small and thus can be neglected.

In what follows the calculated frequency-response at frequency ratios ranging between $\lambda / \Omega = 0.003$ and $\lambda / \Omega = 3$, for the four various values of P, will be presented, compared with experimental results and discussed. For each kind of response identical scales will be used for all the various values of P, to ease comparisons. In all the cases the basic collective pitch angle is equal to 4°.

$$\partial(C_\ell / a\sigma) / \partial \phi$$

The roll moment response to roll angle variations, is shown in Fig. 1, for the four cases: P=1.15. 1.28, 1.33 and 1.56. Most of the experimental results are from Ref. 32 and are marked by open circles. For P=1.15 additional results from Ref. 33, that are marked by asterisks, are also presented.

Three kinds of curves of numerical results are plotted:
a) Results of a complete unsteady aerodynamic model that includes all the effects. It will be denoted model A in what follows.
b) Results of a model that does not include induced velocity variations. It will be denoted B in what follows.
c) Results of a model that includes only the induced velocity variations due to perturbations in the circulation of the trailing vortices (without taking into account shed vortices in the near and far fields, bound vortices of other blades or geometric effects). This model will be denoted model C in what follows.

The third kind of numerical results, model C, was chosen since it was found that the effect of the perturbations in the circulation of the trailing vortices is the most important in most of the cases. In addition, it is agreed among researchers that dynamic-inflow models represent mostly the influence of the trailing vortices. The study included also other combinations of effects that are not presented here, but findings based on these results will be indicated whenever necessary. It should also be pointed out that the unsteady effects are coupled in a highly nonlinear

manner. Thus, for example, the sum of the effects of neglecting shed vortices or neglecting trailing vortices, is not necessarily equal to the effect of neglecting shed and trailing vortices altogether.

As expected, and as indicated in Refs. 32 and 33, the amplitude exhibits two maxima in the neighborhood of the nondimensional resonance frequencies: (P-1), (P+1). The actual maxima (especially the low one) appears at a slightly lower frequency, as expected in a damped system.

At high frequencies there are only small differences between the three theoretical curves of the amplitude. Near the lower maximum, P-1, the results of model B are lower, sometimes by more than 7 dB, compared to the complete model A. When the effect of trailing vortices is added, model C, the agreement is significantly improved.

At low frequencies the trends of the amplitude depend on P. For P=1.15 there is a good agreement between models A and B, while the differences increase in the case of model C that gives higher results. For P=1.28 and 1.33 there are fairly large differences between A and B, with smaller differences between A and C, that still reach 3 dB. For P=1.56 the differences between the three curves increase. Investigation shows that neglecting shed vortices at low frequency ratios lead to the deviations between A and C.

There is a good agreement between the experimental amplitude and the complete unsteady model A, for frequency ratios below the first maximum (P-1). At higher frequency ratios the experimental results are higher than the calculated ones. It is indicated in Ref. 32 that the experimental results may be problematic above a frequency ratio of 0.3. Moreover, comparison between the experimental results of the response to pitch angle variations and roll angle variations, shows that there is a tendency of the experimental results to give too high values (above the correct value) because of problems with the experimental procedure.

The phase angles for the various values of P are presented on the right column of Fig. 1. In each case four regions can be defined:
a) Low frequencies where models B and C agree very well, but differ from model A that gives lower results. These differences increase with P and they are the result of geometric effects.
b) Higher frequencies were model A gives results that are higher than those of models B and C, with model B being the lowest. The differences between models B and A increase with P, while C approaches A. Differences of more than 20° exist between models A and C, with much higher differences appearing between A and B.
c) Higher frequencies where A and C are very close and lower than B.
d) High frequencies where there is a good agreement between all the models.
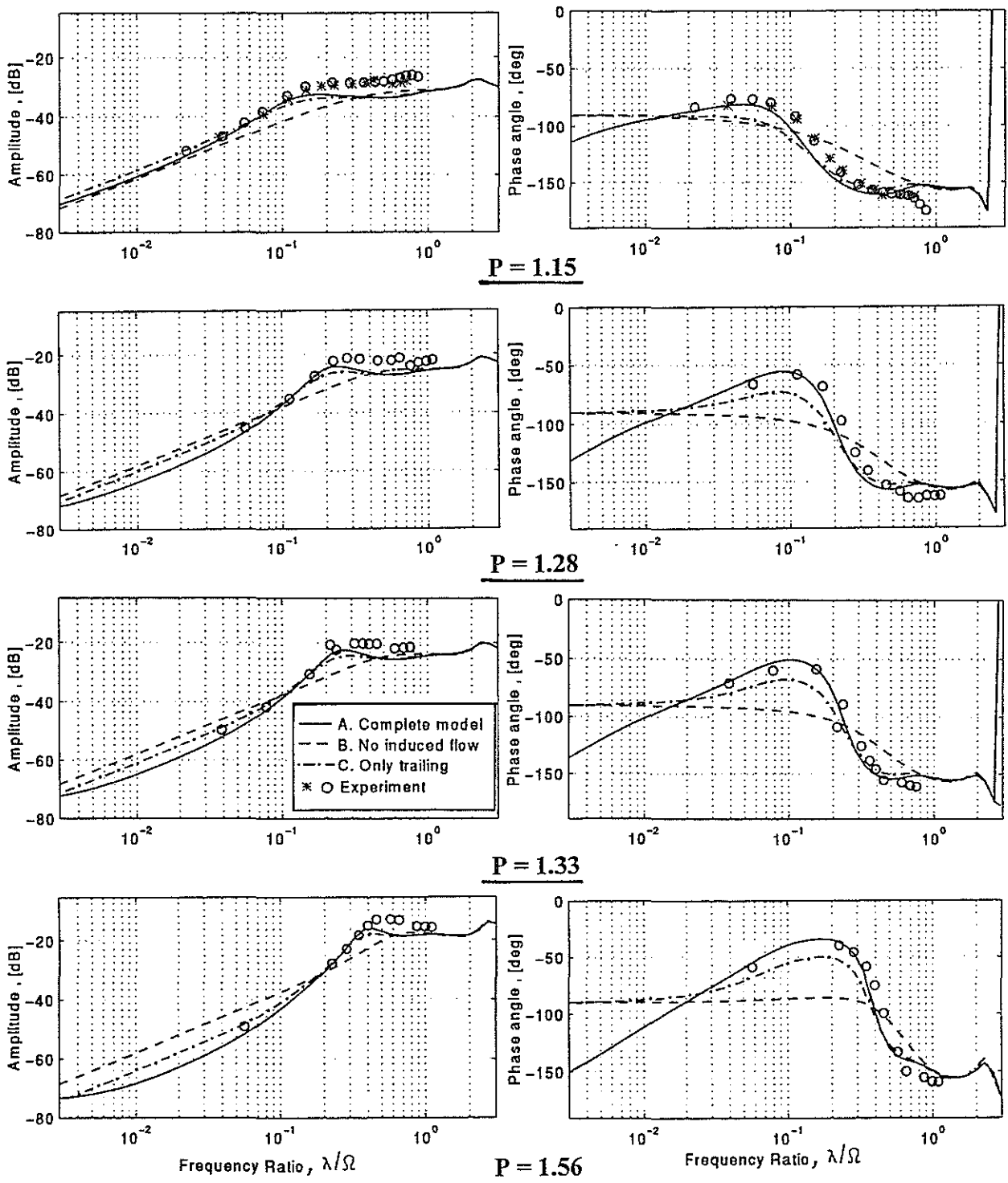
Fig. 1. The frequency-response of the roll moment to roll oscillations, $\partial(C_{\ell} / a\sigma) / \partial\phi$.

$\partial(C_m / a\sigma) / \partial \phi$

In most cases there is a good agreement between the experimental phase angles and the results of the complete model A, except for high frequency ratios for the case P=1.15, where the angles decrease rapidly in the experiment but not according to theory.

The pitch moment response to roll angle variations, an off-axis response, is shown in Fig. 2 for the four values of P.

As in Fig. 1, at high frequencies there is a good agreement between all three models, concerning amplitude and phase angle.
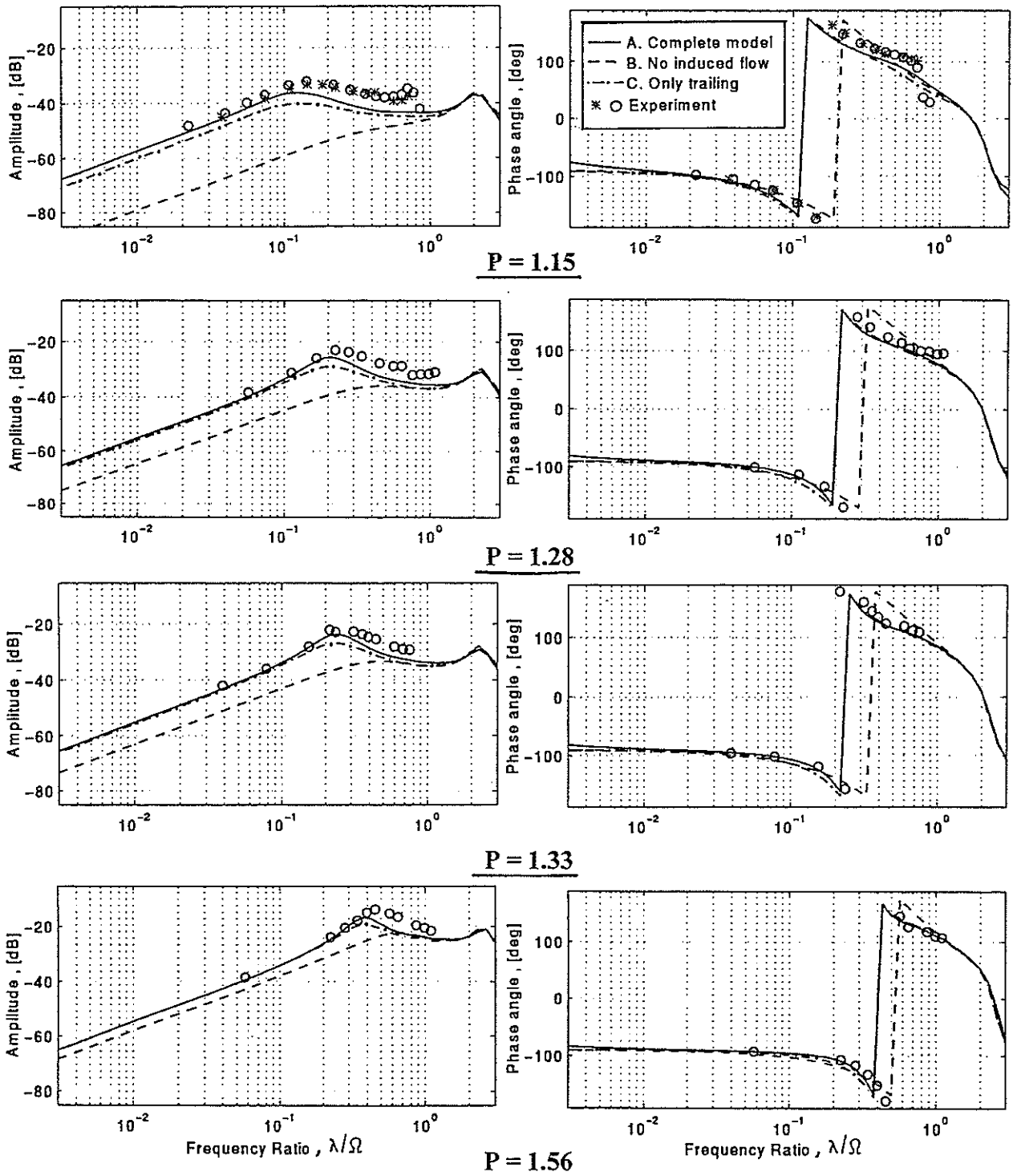
Fig. 2. The frequency-response of the pitch moment to roll oscillations, $\partial(C_m / a\sigma) / \partial\phi$.

In general there is a good agreement between the phase angles obtained using the three models. At phase angles in the neighborhood of 180° there are increasing differences between the phase angles of model B and models A and C (the last two agree nicely where the differences between models A and B exceed 50° for P=1.28 and 1.33).

In the case of the amplitude, for P=1.15, at low and medium frequency ratios, model B is lower than

A by 20 dB,. This difference decreases as P is increased. Model C is also lower than A, but the difference is much smaller (a few dB's for P=1.15) and it almost disappears at higher values of P. Differences still exist near the lower maximum (P-1). It shows that in this case the influence of perturbations in the circulation of the trailing vortices are the most important.

In general there is a good agreement between the experimental amplitude results and model A, except

(as indicated above) for increasing differences in amplitude at high frequencies.

$$\partial(C_m / a\sigma) / \partial\theta_s$$

The pitch moment response to longitudinal cyclic stick command is presented in Fig. 3.

At low frequency ratios model B exhibits relatively small variations of the amplitude as a result of variations of P. On the other hand models A and C predict decreasing amplitudes as P is increased. The differences between A and C at low frequencies increase from 10 dB when P=1.15, to more than 20 dB when P=1.56. The differences between C and A at low frequency ratios decrease from 4 dB at P=1.15, to practically zero at P=1.56.
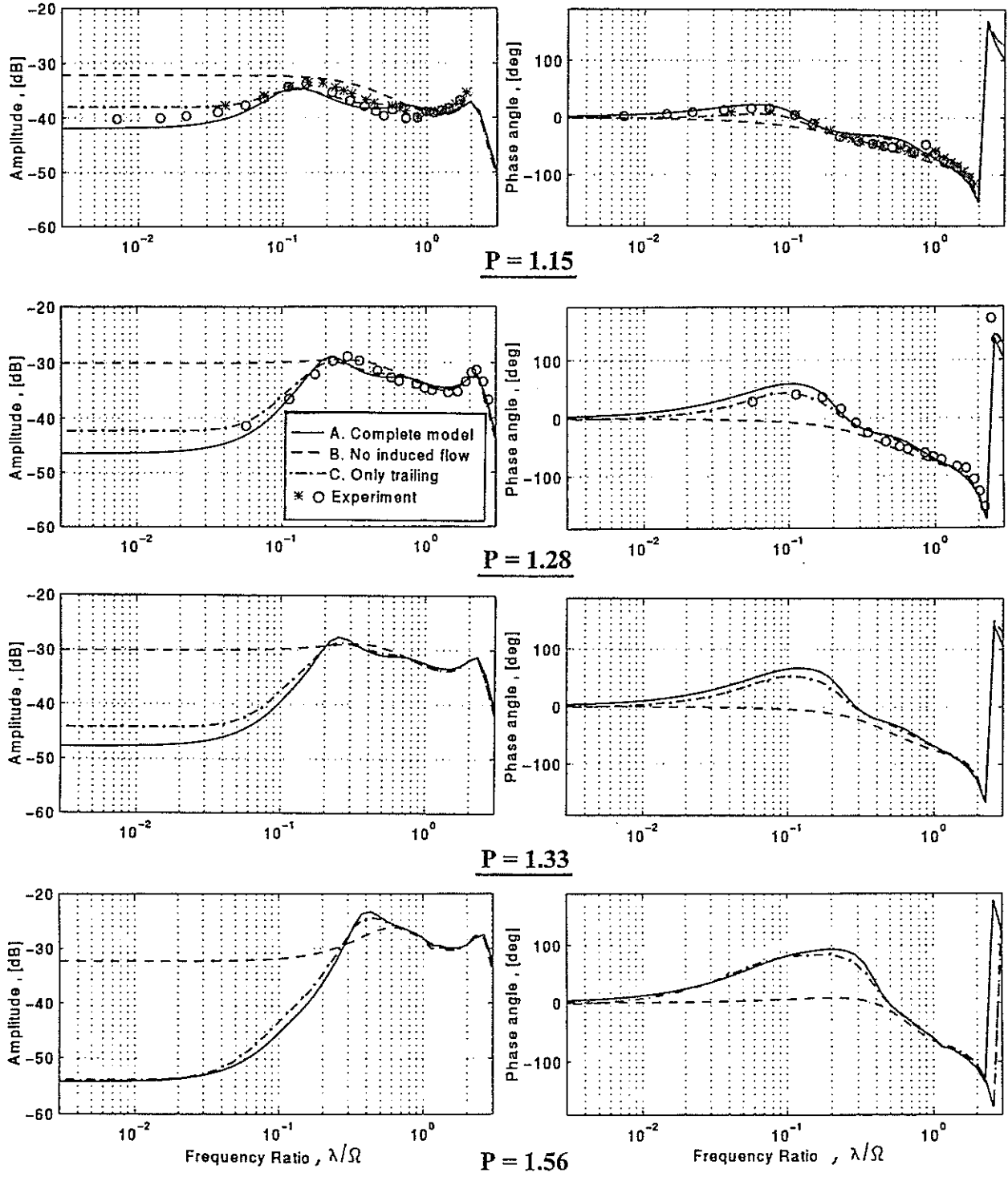
Fig. 3. The frequency-response of the pitch moment to longitudinal stick oscillations, $\partial(C_m / a\sigma) / \partial\theta_s$.

The phase angles obtained from the three models agree at low and high frequency ratios. At intermediate frequency ratios model A gives phase angles higher than model B, with the differences increasing with P and reach 90° for P=1.56. Model C gives phase angles that are slightly lower than those of model A.

Experimental results exist only for P=1.15 and 1.28. There is a good agreement between the experimental results and the results of models A or C.

$$\partial(C_\ell / a\sigma) / \partial\theta_s$$

The roll moment response to longitudinal cyclic stick command is shown in Fig. 4.

At low frequency ratios there are differences between the results of models A, B and C. While at P=1.15 the results of B are slightly lower than A and those of C slightly higher, at high values of P the results of models B and C are higher than A. For P=1.56 the results of B and C are higher (as compared to model A) by 9 dB and 3 dB, respectively.
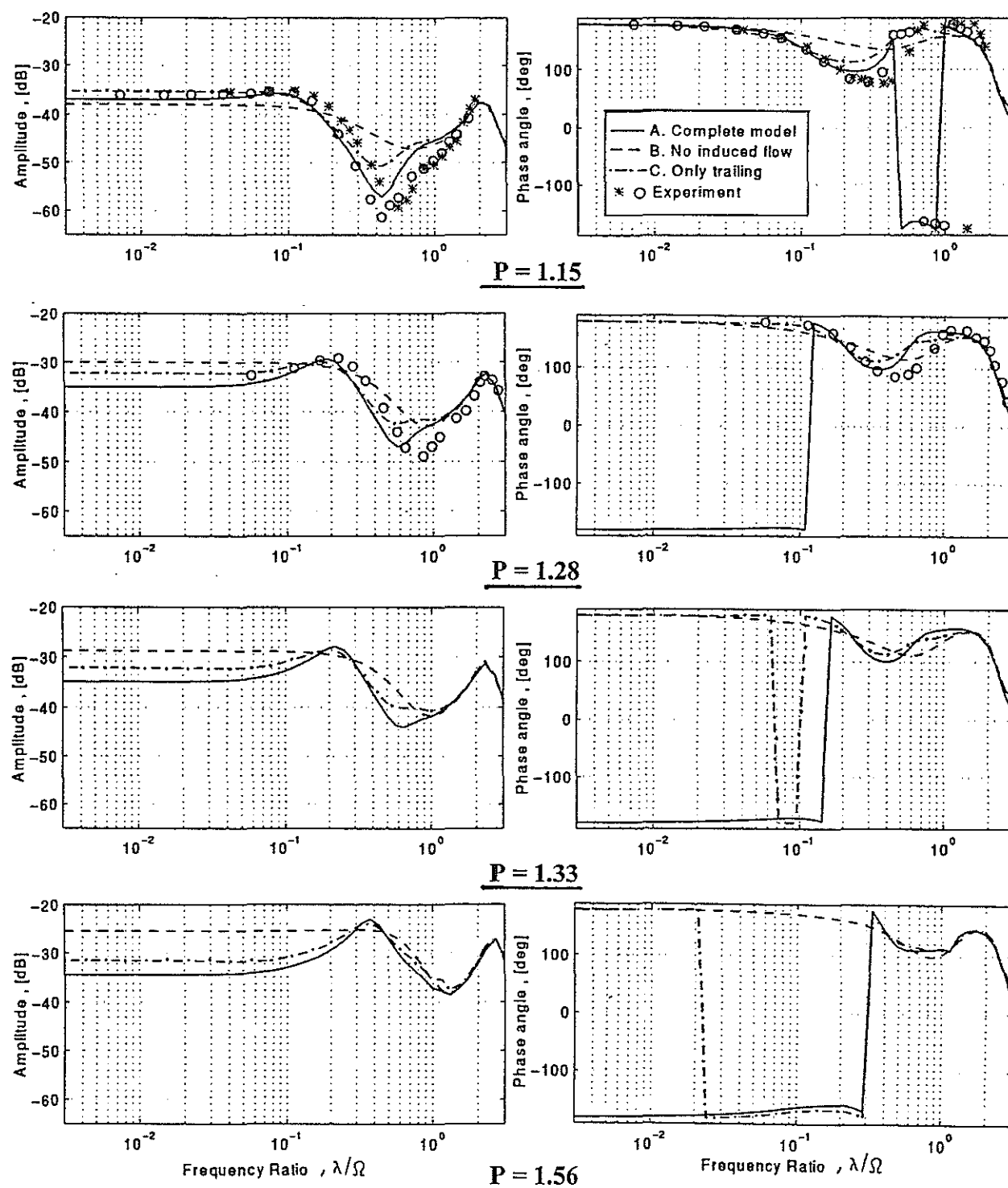
Fig. 4. The frequency-response of the roll moment to longitudinal stick oscillations, $\partial(C_\ell / a\sigma) / \partial\theta_s$.

93.8

There is a clear minimum of the amplitude that occurs at a frequency ratio of 0.4 for P=1.15, and higher frequency ratios as P is increased. For P=1.15 this minimum represents a decrease in amplitude of 20 dB. This decrease is very poorly predicted by model B, while model C still shows a difference of 7 dB in the minimum values. Examination shows that geometric effects and shed vortices have important influences in this case. The minimum becomes less pronounced as P is increased and the differences between the three models decrease at the same time.

In the case of the phase angle there is an agreement between the three models at low and high frequency ratios. At intermediate frequency ratios there are differences that increase as P decreases. For P=1.15 there are differences of up to 40° and 20° between the phase angles as predicted by model A, and models B or C, respectively.

There is in general a good agreement between the experimental results and those of model A, note especially the minimum for P=1.15. It seems that there is a certain shift in predicting the location of the minimum for P=1.28.

4. Conclusions

In general unsteady aerodynamic effects have a large influence on the frequency-response of a hovering rotor. The nature and magnitude of the influence of unsteady aerodynamic effects depend largely on:
• The rotor stiffness (the ratio between the first rotating flapping frequency and the rotor angular speed).
• The frequency of the perturbations.
• The kind of perturbations (shaft oscillations or cyclic pitch oscillations).
• The kind of response (pitch or roll moment).

Only at fairly high frequencies, in the neighborhood of the rotor angular speed and above, unsteady aerodynamic effects become insignificant and models that do not include variations of the induced velocity give good results.

In general perturbations in the circulation of the trailing vortices have the largest influence among the various unsteady effects that include also: shed vortices, geometric effects, bound vortices of the other blades and the near wake. In many cases only the inclusion of the effect of the trailing vortices gives very good agreement with the complete unsteady model. Yet, there are many cases where the inclusion of this effect is not sufficient and the influence of other effects become large.

The complete unsteady aerodynamic model exhibits in general good agreement with experimental results for hingeless rotors that were published in the literature.

References

1) Padfield, G.D., "Helicopter Flight Dynamics: The Theory and Application of Flying Qualities and Simulation Modeling", AIAA Education Series, 1995, 514 pp.

2) Tischler, M.B. and Cauffman, M.G., "Frequency-Response Method for Rotorcraft System Identification: Flight application to BO 105 Coupled Rotor/Fuselage Dynamics", J. of the American Helicopter Society, Vol. 37, No. 3, 1992, pp. 3-17.

3) Tischler, M.B., Driscoll, J.T., Cauffman, M.G. and Freedman, C.J., "Study of Bearingless Main Rotor Dynamics from Frequency-Response Wind Tunnel Test Data", American Helicopter Society Aeromechanics Specialists Conference, San Francisco, CA, Jan. 19-21, 1994, pp. 6.3-1-6.3-25.

4) Bielawa, R.L., "Rotary Wing Structural Dynamics and Aeroelasticity", AIAA Education Series, 1994, 562 pp.

5) Loewy, R.G., "A 2-D Approximation to the Unsteady Aerodynamics of Rotary Wings", J. of Aero. Sci., Vol. 24, No. 2, 1957, pp. 81-92.

6) Ham, N.D., Moser, H.H. and Zvara, J., "Investigation of Rotor Response to Vibratory Aerodynamic Inputs - Parts I. Experimental Results and Correlation with Theory", WADC Technical Report 58-87, Part I, October 1958, 43 pp.

7) Silveria, M. and Brooks, G.W., "Dynamic-Model Investigation of the Damping of Flapwise Bending Modes of Two-Blade Rotors in Hovering and a Comparison with Quasi-Static and Unsteady Aerodynamic Theories", NASA TN D-175, 1959, 30 pp.

8) Kato, K., Yamane, T., Nagashima, T., Iboshi, N. and Yamagishi, K., "Experimental Substantiation for Hovering Rotor Vertical Impedance Calculations", J. of Aircraft, Vol. 18, No. 6, 1981, pp. 445-450.

9) Nagashima, T., Hasegawa, G., Nekohashi, T. and Hirose, T., "Aeroelastic Response Characteristics of a Rotor Executing Arbitrary Harmonic Blade Pitch Variations", 14th European Rotorcraft Forum, Milan, Italy 20-23 September, 1988, Paper 61.

10) Gaonkar, G.H. and Peters, D.A., "Review of Dynamic Inflow Modeling for Rotorcraft Flight Dynamics", Vertica, Vol. 12, No. 3, 1988, pp. 213-242.

11) Peters, D.A., Boyd, D.D. and He, C.J., "Finite-State Induced-Flow Model for Rotors in Hover

and Forward Flight", *J. of the Am. Helicopter Soc.*, Vol. 34, No. 4, 1989, pp. 5-17.

12) Ormiston, R.A. and Peters, D.A., "Hingeless Helicopter Rotor Response with Nonuniform Inflow and Elastic Blade Bending", *J. of Aircraft*, Vol. 9, No. 10, 1972, pp. 730-736.

13) Gaonkar, G.H. and Peters, D.A., "Effectiveness of Current Dynamic-Inflow Models in Hover and Forward Flight", *J. of the American Helicopter Society*, Vol. 31, No. 1, 1986, pp. 47-57.

14) Crews, S.T. and Hohenemser, K.H., "An Unsteady Wake Model for a Hingeless Rotor", *J. of Aircraft*, Vol. 10, No. 12, 1973, pp. 758-760.

15) Curtiss, H.C. Jr., "On the Calculation of the Response of Helicopters to Control Inputs", 18th European Rotorcraft Forum, Avignon, France, Sept. 14-17, 1992, Paper F07.

16) Rosen, A. and Isser, A., "A New Model of Rotor Dynamics During Pitch and Roll of a Hovering Helicopter", *J. of the American Helicopter Society*, Vol. 40, No. 3, 1995, pp. 17-28 (also Proceedings of the 50th Annual Forum of the American Helicopter Society, Washington, D.C., May 11-13, 1994, pp. 409-426).

17) Arnold, U.T.P., Keller, J.D., Curtiss, H.C. and Reichert, G., "The Effect of Inflow Models on the Dynamic Response of Helicopters", 21st European Rotorcraft Forum, Saint Petersburg, Russia, Aug. 30- Sept. 1, 1995, Paper VII-8.

18) Keller, J.D., "An Investigation of Helicopter Dynamic Coupling Using an Analytical Model", *J. of the American Helicopter Society*, Vol. 41, No. 4, 1996, pp. 322-330.

19) Leishman, J.G. and Nguyen, K.Q., "State Space Representation of Unsteady Airfoil Behavior", *AIAA J.*, Vol. 28, No. 5, 1990, pp. 836-844.

20) Turnour, S.R. and Celi, R., "Effects of Unsteady Aerodynamics on the Flight Dynamics of an Articulated Rotor Helicopter", *J. of Aircraft*, Vol. 34, No. 2, 1997, pp. 187-196.

21) Fletcher, J.W., "Identification of Linear Models of the UH-60 in Hover and Forward Flight", 21st European Rotorcraft Forum, Saint Petersburg, Russia, Aug. 30 - Sept. 1, 1995, Paper VII-4.

22) Mansur, H.M. and Tischler, M.B., "An Empirical Correction Method for Improving Off-Axes Response Prediction in Component Type Flight Mechanics Helicopter Models", AGARD Flight Vehicle Integration Panel Symp. on Advanced Rotorcraft Technology, Ottawa, Canada May 27-30, 1996, Paper A22.

23) Rosen, A. and Isser, A., "The Influence of Variations in the Locations of the Blades on the Loads of a Helicopter Rotor During Perturbations About an Axial Flight", TAE Report No. 721, Technion-I.I.T., Faculty of Aerospace Eng., Oct. 1994, 94 pp.

24) Isser, A. and Rosen, A., "A Model of the Unsteady Aerodynamics of a Hovering Helicopter Rotor that Includes Variations of the Wake Geometry", *J. of the American Helicopter Society*, Vol. 40, No. 3, 1995, pp. 6-16 (also Proceedings of the 34th Israel Annual Conference on Aerospace Sciences, Feb. 1994, pp. 90-105).

25) Rosen, A. and Isser, A., "Investigation of the Technion Model of Unsteady Rotor Aerodynamics (TEMURA)", presented at the 6th International Workshop on Dynamics and Aeroelastic Stability Modeling of Rotorcraft Systems, University of California, Los Angeles (UCLA), Nov. 8-10, 1995.

26. Rosen, A., Isser, A. and Yoshpe, M., "The Influence of Unsteady Aerodynamics and Inter-Blade Aerodynamic Coupling on the Blades Response to Harmonic Variations of Their Pitch Angles", *The Aeronautical J.*, Vol. 100, No. 991, 1996, pp. 27-35.

27) Rosen, A. and Isser, A., "A New Unsteady Aerodynamic Model of the Coupled Rotor-Body Dynamics", American Helicopter Society 51st Annual Forum, Fort Worth, Texas, May 9-11, 1995, Vol. 2, pp. 1763-1787.

28) Rosen, a. and Isser, A., "The Influence of Unsteady Aerodynamic Effects on the Coupled Free Vibrations of Rotor Flapping and Body Pitch and Roll in Hover", *J. of the American Helicopter Society*, Vol. 41, No. 3, 1996, pp. 208-218.

29) Isser, A. and Rosen, A., "The Pitch Damping of a Hovering Rigid Rotor", *J. of the American Helicopter Society*, Vol. 42, No. 1, 1997, pp. 96-99.

30) Rosen, A. and Isser, A., "A New Unsteady Aerodynamic Model of the Coupled Rotor-Body Dynamics", TAE Report No. 728, Faculty of Aerospace Eng., Technion-I.I.T., March, 1995, 115 pp.

31) Kuczynski, W.A. and Sissingh, G.J., "Characteristics of Hingeless Rotors with Hub Moment Feedback Controls Including Experimental Rotor Frequency-Response", Report LR 25048 Lockheed-California Co., Burbank, CA, Jan. 1972, 130 pp.

32) Kuczynski, W.A., "Experimental Hingeless Rotor Characteristics at Full Scale First Flap Mode Frequencies (Including Rotor Frequency-Response to Shaft Oscillations)", Report LR 25491, Lockheed-California Co., Burbank, CA, Oct. 1972, 236 pp.

33) London, R.J., Watts, G.A. and Sissingh, G.J., "Experimental Hingeless Rotor Characteristics at Low Advance Ratio with Thrust", NASA CR-114684, Lockheed-California Co., Burbank, CA, Dec. 1973, 206 pp.